Frontiers in Emerging Engineering & Technologies (Open Access)

Volume 03, Issue 06, June 2026,
DOI: - https://doi.org/10.64917/feet/Volume03Issue06-01 PageNo.14-28

Statistical Analysis of Failure Incidence and Pipeline Repair Planning Based on In-Line Inspection Data

Ilnar Iakhin
Independent researcher, Novy Urengoy, Russia

RECEIVED - 21-04-2026, **RECEIVED REVISED VERSION** - 19-05-2026, **ACCEPTED**- 17-06-2026, **PUBLISHED**- 30-06-2026

Abstract

This article presents a seven-year empirical analysis (2019–2025) of an in-line inspection (ILI) dataset from an Arctic gas-gathering network. The work integrates failure-incidence statistics with probabilistic risk-based modelling to quantify the latent risk contained in the backlog of deferred category B defects, an analytical step undocumented for deep-reservoir permafrost infrastructure. The relevance stems from aging pipeline assets, the operating conditions of gas-gathering systems linked to deep high-pressure gas-condensate reservoirs in the Arctic cryolithozone, and the limits of deterministic approaches insensitive to instrumental error and variability in metal-degradation rates. The aim is to refine repair-planning approaches based on empirical ILI data. The novelty lies in the synthesis of a seven-year diagnostic dataset (380 defects: 40 category A and 340 category B) with probabilistic risk-based maintenance models. Elastic-plastic bends dominate the population (82%) alongside carbon-dioxide corrosion. Across 2019–2025 the cumulative elimination rate reached 80% for category A (32 of 40) and 6.8% for category B (23 of 340), leaving 317 unresolved anomalies. Monte Carlo projections indicate 5.1% of this backlog will exceed the 300 mm deflection threshold within three years and 10.0% within five years. Bayesian analysis flags 20 defects as misclassified through ILI tool uncertainty alone.

Keywords: pipeline integrity management; in-line inspection; risk-based maintenance; Monte Carlo simulation; Bayesian analysis; Arctic permafrost pipelines

Abbreviations

AI – Artificial Intelligence

ALARP – As Low as Reasonably Practicable

Cat A – Category A

Cat B – Category B

CDF – cumulative distribution function

CoF – Consequence of Failure

EPB – Elastic-Plastic Bend

FORM – First-Order Reliability Method

ILI – in-line inspection

MFL – magnetic flux leakage

ML – machine learning

Psw – safe operating pressure parameter

PoF – Probability of Failure

SHAP – SHapley Additive exPlanations

1. Introduction

Ensuring the reliability, structural integrity, and environmental safety of gas-gathering pipelines operating in Arctic permafrost conditions represents one of the most technically demanding problems in contemporary pipeline integrity management, with direct consequences for energy supply continuity, environmental protection, and operating cost control (Khan et al., 2021). Trunk and field pipelines represent critical infrastructure subject to operational loads, aggressive multiphase transported media, and adverse external geomechanical factors (Ismayilov et al., 2021). Under conditions of aging infrastructure assets and the gradual shift of hydrocarbon production toward deep-lying horizons with extreme conditions, traditional methods of preventive and reactive maintenance exhibit increasing economic and technological limitations (Babayeju et al., 2024). This leads either to unjustified capital expenditures on excessive inspections and repairs or, conversely, to sudden equipment failures entailing catastrophic consequences (Mardanov et al., 2025).

This problem acquires particular scientific and practical relevance in the operation of field pipelines associated with deep, high-pressure gas-condensate reservoirs operating under Arctic cryolithozone conditions. Such reservoirs are characterized by pressures approaching 60 MPa, temperatures exceeding 106 °C, and an elevated partial pressure of carbon dioxide above 0.21 MPa. Such thermobaric conditions and the physicochemical composition of the fluid act as catalysts of carbon dioxide corrosion. This, along with intense geodynamic processes in the permafrost soils of the cryolithozone, is the principal cause of steel pipeline degradation (Wang et al., 2023). According to international statistics, corrosion damage and geomechanical deformations account for more than 40% of all incidents involving loss of containment in the oil and gas sector (Parlak and Yavasoglu, 2023).

Modern pipeline operators determine the state of their asset and plan its repair/reinforcement using deterministic models such as ASME B31G and DNV-RP-F101, which reduce multi-dimensional arrays of in-line inspection data to a single worst-case defect calculation using fixed safety factors (Omolegbe, 2026). As a result, the final decision becomes binary (repair / do not repair), which ignores the instrumental error of inspection tools, the variation of defect growth rates, and local variation of operational parameters affecting the performance of hardware components. As a consequence, operators encounter the phenomenon of accumulation of deferred category B defects while simultaneously expending resources inefficiently on eliminating false-positive anomalies (Omolegbe, 2026).

In this connection, the research problem is formulated as a contradiction between the growing complexity of operating conditions in the gas-gathering networks of deep Arctic gas-condensate reservoirs, which generate arrays of complex interacting defects such as elastic-plastic bends and local corrosion, and the insufficient flexibility of the applied deterministic repair prioritization algorithms, which are incapable of predictive risk analysis.

The aim of the study is to improve the substantiation of decisions on field pipeline integrity management by refining approaches to failure incidence assessment, defect formation analysis, and repair planning based on in-line inspection (ILI) results for 2019–2025.

To achieve this aim, the following objectives are addressed in the study:

1. To perform a quantitative and qualitative analysis of the empirical ILI data array for the identification of category A defects (critical) and category B defects (subject to monitoring).
2. To assess the practice of applying of the standard in the context of hazard rank calculation and repair method selection.
3. To analyze the physical-mechanical and chemical root causes of dominant defects on the basis of specific case studies.
4. To substantiate the necessity of introducing probabilistic models and machine-learning algorithms to overcome the barriers of deterministic planning.

The scientific novelty of the work lies in the original synthesis of large-scale empirical ILI data covering a seven-year operating period for a unique gas-condensate asset, using advanced global risk-based maintenance concepts. Using detailed metrics, it is demonstrated how the limitations of traditional physical degradation models can be mitigated by integrating Bayesian data updating and stochastic forecasting, thereby transforming reactive infrastructure maintenance into proactive maintenance.

2. Materials and Methods

To conduct the study, a methodological framework was formed that combines quantitative statistical analysis, case studies, content analysis of regulatory and technical documentation, and a review of contemporary specialized literature. To preserve confidentiality and avoid identification of the operator and asset, the names of the field, production units, and well clusters are anonymized or generalized throughout the paper. The technical characteristics relevant to the analysis are retained in an aggregated and non-identifiable form. The empirical basis of the study consisted of data on category A and category B defects identified during in-line inspections of an operating field gas-gathering system for the period 2019–2025. The array includes aggregated data for 2019–2022 and separate samples for 2023, 2024, and 2025. In total, 380 defects were analyzed, including 40 category A defects and 340 category B defects. According to the appendices, 55 defects were eliminated, and 325 were not, which makes it possible to use the array not only for descriptive characterization of defectiveness but also for analyzing repair-prioritization practices.

Comparative and statistical analysis. The principal knowledge-extraction instrument consisted of processing raw data arrays obtained during runs of in-line inspection tools. Within this approach, the frequency distributions of defects by type, as well as their geometric and diagnostic parameters, were analyzed: distance along the route, bend radius, bend deflection, longitudinal and transverse dimensions of metal loss, defect depth, calculated safe operating pressure of the pipe with a defect, and hazard rank. According to the empirical data, elastic-plastic bends dominate in the studied population: 312 cases, or approximately 82% of all recorded defects. Girth weld anomalies (26 cases), dents (14), mechanical damage (11), and corrosion defects (10) are considerably less frequent. Category A defects are characterized by a relatively high elimination rate (32 of 40, or 80%), whereas only 23 of 340 category B defects (about 6.8%) were eliminated, indicating pronounced asymmetry in repair practice and confirming the determining role of the prioritization system.

Content analysis of technical documentation. A study was conducted of corporate protocols for information entry and repair prioritization. In particular, the decision-making mechanism embedded in the standard of the rules for determining the technical condition of main gas pipelines based on the results of in-pipe inspection (hereinafter referred as standard), regulating the sequence of routing trunk and field gas pipeline sections into repair, was deconstructed. Analysis of the attached documentation showed that not only the primary defect parameters according to ILI data, but also the calculated indicators Psw, hazard rank, and elimination priority must be entered into the database. The prioritization criteria are formalized as follows: Priority 1 includes defects with a depth of 50% or more or with a hazard rank above 1.0; Priority 2 includes defects with a depth of 30–50% or with a rank of 0.5–1.0; Priority 3 includes defects with a depth of up to 30% or with a rank of up to 0.5. This enabled associating the statistical distribution of defects with the organizational and regulatory logic of repair decision-making.

Case studies. To illustrate the nonlinear physics of failure processes, a method of deep analysis of specific precedents of defect formation was applied. As benchmark cases, three representative locations within the studied field pipeline network were selected, hereafter referred to as Site A, Site B, and Site C, together with adjacent sections identified in the empirical array as exhibiting extreme deformation states. The selection of these cases is due to the fact that it is precisely there that combinations of significant elastic-plastic bends, welded-joint anomalies, and local corrosion damage are recorded, which makes possible an analysis of the combined influence of pipeline geometry, stress-strain state, and operating factors on defect development.

Probabilistic modelling framework. To quantify the latent risk embedded in the category B backlog, four probabilistic analyses were applied directly to the empirical dataset. First, a two-parameter Weibull distribution and a lognormal distribution were fitted to the bend-deflection measurements of category B EPB records (n = 275; one instrument-range observation exceeding 2000 mm was excluded as an MFL tool-range artifact, yielding a working sample of n = 274) using maximum-likelihood estimation, and goodness of fit was assessed by the Kolmogorov–Smirnov test. Second, a Monte Carlo simulation (10,000 iterations per defect) was conducted for the 244 category B EPB records with deflection below the 300 mm reclassification threshold. Annual deflection growth was treated as a lognormal random variable parameterised from published geomechanical data for permafrost environments (Wang et al., 2023); where paired measurements of the same defect across successive ILI cycles were available in the dataset, the empirically derived growth increments were used to cross-validate the assumed parameter range (see Section 3.5). Third, a Bayesian misclassification analysis was performed by propagating the declared ILI tool uncertainty of ±15% through the category boundary at 150 D to identify defects whose true radius may fall below the critical threshold despite a non-critical recorded value. Fourth, a temporal risk-accumulation estimate was derived by combining the trend data from the statistical profile with the Monte Carlo exceedance projections.

Software and reproducibility. All statistical computations, distribution fitting, goodness-of-fit testing, Monte Carlo simulation, and Bayesian posterior updating were implemented in Python 3.11 using the scipy.stats (v1.11), numpy (v1.26), and pandas (v2.1) libraries. Pseudo-random-number generation used the PCG64 bit generator seeded with a fixed value (seed = 42) for full reproducibility. For each of the 244 category B EPB defects with deflection below 300 mm, annual growth increments were drawn from a lognormal distribution with mean $\mu_g = 0.08$ and standard deviation $\sigma_g = 0.04$, applied multiplicatively to the measured deflection over a five-year horizon (ten thousand independent trajectories per defect). Exceedance probability was computed as the fraction of trajectories crossing the 300 mm threshold at each annual step. For Bayesian posterior updating, the likelihood function adopted a Gaussian measurement model centred on the reported radius with $\sigma = 7.5\%$ of the reported value (corresponding to the declared ±15% ILI tool uncertainty at the 95% confidence level), and a uniform non-informative prior over the admissible radius range. Anonymised aggregated data and the analysis scripts are available from the author upon reasonable request, subject to the confidentiality arrangement described in the Data availability statement.

Literature review. The empirical results were integrated with contemporary scientific conceptions on the development of non-destructive testing technologies, the mathematical modeling of failure probability, and the digital transformation of the oil and gas sector. This made it possible to interpret the patterns identified in the array as manifestations of broader industry trends, a transition from reactive elimination of individual damage to risk-based management of the technical condition of pipeline systems.

3. Results

3.1. Contextualization with contemporary literature

Recent scholarship on pipeline integrity management links the sector's current development path with a shift toward data-driven architectures in which in-line inspection, risk assessment, and machine learning are integrated into a single decision cycle (Bastek et al., 2026). Reviews of sensing systems and corrosion forecasting show that the key challenge now lies in data fusion, signal interpretation, and conversion of diagnostic outputs into inspection and repair actions, which places machine learning inside the engineering workflow itself (Olawole et al., 2026). A systematic review of machine-learning applications to pipeline networks identifies the same constraints that matter for oil and gas infrastructure, including weak feature standardization, heterogeneous failure archives, and limited model transferability across assets and operating regimes (Chen et al., 2025).

The probabilistic branch of the literature shifts the analytical focus from a single calculated defect to a network of causal dependencies in which corrosion, environmental exposure, measurement quality, and operating conditions are represented within one risk model (Soomro et al., 2022). For gas pipelines with multiple leakage drivers, dynamic Bayesian networks have been used to build time-evolving risk models that can be updated as new inspection data and operational events become available (Wang et al., 2025). A similar direction appears in studies of external corrosion, where dynamic Bayesian network models support temporal failure assessment and provide a basis for revising inspection priorities and protective measures as the condition state changes (Wu et al., 2025).

A separate stream of research addresses the quality of ILI data itself, since measurement error, outliers, and incorrect matching of defects across inspection cycles alter the full logic of remaining-life prediction (Hussain and Zhang, 2024). For corrosion-depth forecasting, ensemble Bayesian neural network models have been proposed to generate both point predictions and uncertainty distributions, while SHAP-based interpretation reveals the contribution of environmental and geometric variables to defect growth (Cui and Wang, 2024). The problem of matching defects between successive ILI runs has also received dedicated attention in work on probabilistic defect alignment and pitting-growth prediction, where reliable tracking of the same corrosion feature across time becomes the foundation for maintenance planning and residual-life estimation (Verdín Martinez et al., 2026).

Statistical studies of corrosion defects indicate that real pipeline populations often follow mixed distributional regimes shaped by fluid composition, service life, and the circumferential location of metal loss on the pipe wall (Velázquez et al., 2024). For complex corrosion morphologies, researchers have combined Monte Carlo simulation with FORM and explicit treatment of river-bottom profiles, showing that local route geometry changes the stress field and therefore the estimated limit state of the pipe (Motta et al., 2024). Related work on API 5L pipeline reliability and failure-pressure prediction for complex corrosion through deep learning points toward unified models in which defect statistics and fracture mechanics inform a single predictor of residual strength and failure risk (Zelmati et al., 2025; Shahgholian-Ghahfarokhi et al., 2026).

For pipelines in permafrost regions, recent literature connects deformation risk with heat transfer from the pipe to frozen soils, talik formation, and differential settlement of the foundation, all of which reshape the stress state along extended sections of the line (Cao Y. et al., 2024). The next stage in this line of work focuses on engineering adaptation, including a powerless ventilation technique for buried pipelines that reduces thaw settlement and stabilizes the thermal regime around the pipe (Cao Y. et al., 2025). For design and operational practice, framework-based methods for thaw-settlement assessment and recent reviews of machine-learning models for permafrost degradation are also important, since they convert dispersed geotechnical and climatic data into infrastructure vulnerability maps and adaptation scenarios (Mohammadi and Hayley, 2026; Memiş et al., 2025).

3.2. Statistical profile of defect formation and failure incidence for 2019–2025

Analysis of the consolidated ILI dataset for the studied gas-gathering pipeline network reveals a complex picture of asset technical condition, uneven in time and space. The defects are strictly stratified: category A represents critical damage requiring immediate routing of the section for repair due to an unacceptable reduction in the pipe's load-bearing capacity. Category B includes defects that are recorded and entered into the database, but permit continued operation under monitoring or are subject to scheduled elimination in the long term. Summary results of the detection and elimination status of defects by year are presented in Table I.

Table I. *Summary statistics on the detection and elimination of defects in gas collection manifolds based on the results of the technical inspection for 2019–2025.*

ILI Period	Cat A Identified	Cat A Eliminated	Cat A Elim. Rate	Cat B Identified	Cat B Eliminated	Cat B Backlog (not elim.)	Cat B Elim. Rate	Dominant Defect Types
2019–2022	14	13	**93%**	136	20	**116**	15%	EPB: 10; Corrosion: 1; Dent/Mech: 2; Delam.: 1
2023	17	13	**76%**	78	0	**78**	0%	EPB: 15; Dent/Weld: 1; Girth-weld anom.: 1
2024	6	6	**100%**	82	3	**79**	4%	EPB: 4; Corrosion: 2 (EPB: 65; Corros.: 7)
2025 (thru Oct.)	3	0	**0%†**	44	0	**44**	0%†	EPB: 3 (EPB: 44)
TOTAL	**40**	**32**	**80%**	**340**	**23**	**317**	**6.8%**	**EPB dominant (82% of all defects)**

† 2025 data are partial (through October); the elimination campaign for identified defects was ongoing at the time of analysis. The headline elimination rate of 80% (32/40) is computed over the full 2019–2025 period including ongoing 2025 work; for completed periods (2019–2024) only, the category A elimination rate is 86.5% (32/37). Defect-type counts for Cat B shown in parentheses where distinct from Cat A. EPB = Elastic-Plastic Bend; Delam. = Delamination; Girth-weld anom. = girth-weld anomaly.

The data in Table I demonstrate the problem of integrity management: against the background of high promptness in eliminating critical threats, where 32 of 40 category A defects were eliminated (elimination rate: 80%), an avalanche-like accumulation of category B defects occurs. 317 category B defects remain in the 'Not eliminated' status. Within the framework of reliability theory, this forms a large-scale pool of latent risk, since any category B defect, under changing operating conditions or external influences, has a mathematical probability of progressing to an emergency condition.

Additionally, it was established that the ILI materials recorded bends with radii of approximately 49–150 D for category A defects and 154–438 D for category B defects, with bend deflections ranging from 7.58 mm to values exceeding 1500 mm. Statistical analysis of the full population reveals a sharp bimodal separation by bend radius between the two categories: the mean bend radius for category A defects is 122.3 D (median 131.0 D, $\sigma = 26.3$ D), while for category B the mean is 249.6 D (median 252.0 D, $\sigma = 48.4$ D). A Mann–Whitney U-test confirms that the two distributions are fully non-overlapping ($U = 0$, $p < 0.001$), indicating that bend radius alone constitutes a near-perfect classifier of hazard category within this dataset and that the deterministic threshold embedded in the standard captures the extreme tail of the distribution, but provides no gradation within the wide intermediate zone. Note that bend-radius statistics are computed exclusively for EPB-type defects; the Cat A subsample comprises $n = 30$ rather than all 32 Cat A EPB records because two entries lacked a valid radius measurement in the ILI report and were excluded from the distributional analysis. Similarly, the Cat B subsample of $n = 275$ excludes one EPB record with an implausible radius value flagged as a data-entry error. Frequency distribution of EPB bend radii by hazard category is shown in Figure I.

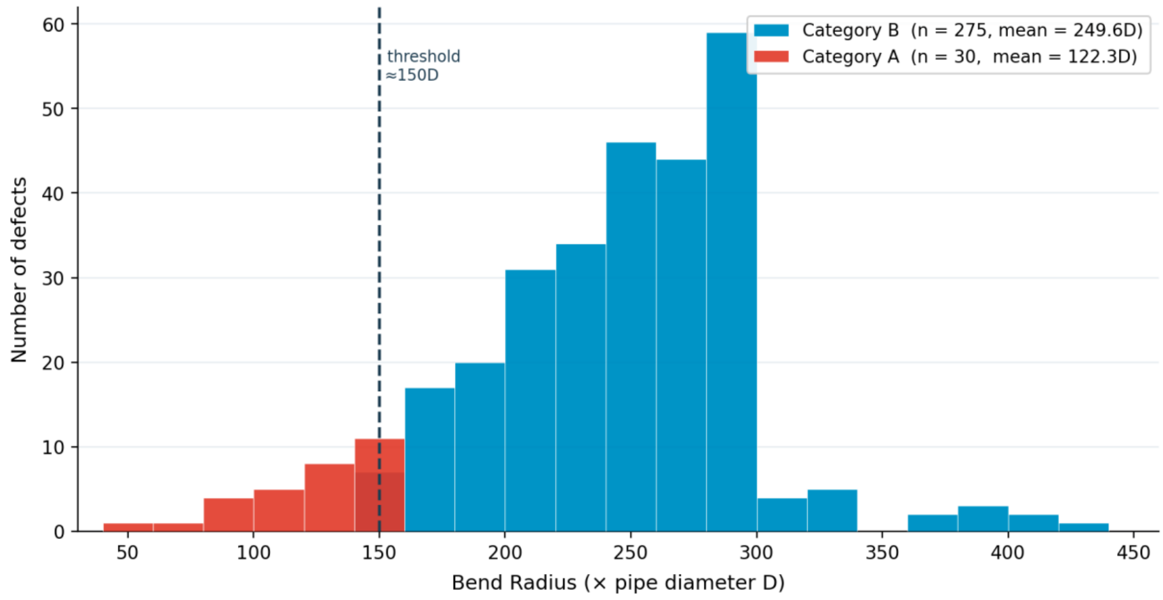

Figure I. *Frequency distribution of EPB bend radii by hazard category (Cat A: n = 30; Cat B: n = 275).*

A temporal trend in defect detection rate is equally noteworthy. The average annual discovery rate of category B defects was 34 per year during 2019–2022, rising sharply to 78 per year in 2023 and 82 per year in 2024. As of October 2025, 44 additional category B defects have been recorded, implying an annualized rate of approximately 53 per year. The cumulative unresolved backlog of category B defects stands at 317 items as of the date of this analysis. This accelerating detection rate, combined with a near-zero elimination rate for category B (6.8% over the entire study period), indicates that the gap between system degradation and remediation capacity is widening structurally rather than cyclically. Annual category B defect detection rate and cumulative unresolved backlog for the period 2019–2025 is shown in Figure II.

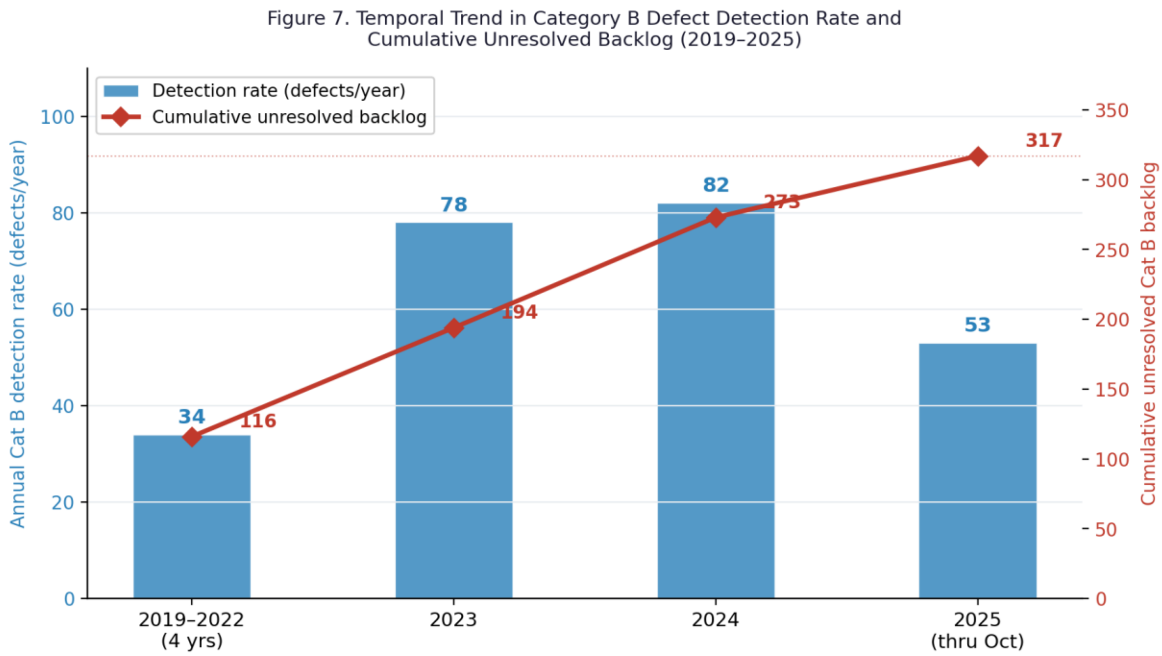

Figure II. *Annual category B defect detection rate and cumulative unresolved backlog for the period 2019–2025.*

The distribution of critical category A defects by the physical nature of their occurrence demonstrates the absolute predominance of the geomechanical factor. 80% of critical incidents (32 out of 40) were classified by the measurement systems as elastic-plastic bends (EPB). Corrosion and mechanical damage each account for 7.5% (3 defects each), while girth-weld anomalies and delamination each represent 2.5% (1 defect each). Such an anomalous concentration of deformation defects directly correlates with the cryolithozone conditions under which the studied gas-gathering pipelines are operated. The thermal effect of the transported high-temperature fluid on permafrost soils leads to the formation of thaw bulbs, or taliks. The settlement of thawing soil deprives the pipeline of support. In winter, reverse processes come into operation: frost heave of water-saturated soils pushes the pipe body upward (Huang et al., 2023). The cyclic action of these oppositely directed geodynamic forces generates bending moments exceeding the yield strength of pipeline steel, usually X60 or X65, transferring the metal into an elastic-plastic state (Youssef et al., 2024).

3.3. Practice of applying the deterministic model of the standard

Analysis of technical documentation enables the decision-making methodology applied by the operator to be deconstructed, based on the standard. The model is strictly deterministic and relies on threshold values for defect geometric parameters.

The planning process is initiated by loading raw ILI data. Within 5 days, the engineering center determines the safe operating pressure parameter and calculates the synthetic indicator, Hazard Rank. Based on the obtained value and the actual depth of pipe wall loss, the defect is assigned to one of three priority categories shown in Table II.

Table II. *Priority categories for defect repair according to the standard.*

Priority Level	Inclusion Criterion (Defect Depth / Hazard Rank)	Response Procedure	Predominant Repair Methods Identified
Priority 1	≥ 50% wall thickness OR rank > 1.0	Repair first	Pipe replacement, cut-out section replacement, excavation work, for ILI-detected defects
Priority 2	30%–50% wall thickness OR 0.5 < rank ≤ 1.0	Repair second	On-stream repair, composite sleeves
Priority 3	30% wall thickness OR rank ≤ 0.5	Repair third	Grinding, monitoring

Comparison of this matrix with actual repair records for 2019–2024 reveals a high degree of correspondence between the type of damage and the implemented physical measure. In the periods 2019–2022 and 2024, all category A defects with a hazard rank above 1.0 were routed into work under Priority 1 within the same operational cycle. In 2023, four category A defects (23.5% of the annual total) remained unresolved at the time of data extraction; review of the corresponding records indicates that these defects were reclassified to a lower hazard rank following re-inspection or engineering reassessment and were consequently deferred to a subsequent repair campaign. This does not affect the overall prioritisation logic of the standard but underscores the need for transparent audit trails when defect status changes between inspection cycles. To eliminate structural failures such as deep corrosion and deep mechanical gouges, the method of cutting out the defective spool piece for cut-out was applied without alternative. However, for the elimination of EPB defects, the principal method consisted of earthworks and trenching. This engineering approach is elegant in its physical essence: excavation of frozen soil in the bend zone relieves the colossal external geomechanical pressure. The released steel stringer, due to accumulated internal potential elastic energy, can partially relax and return to a position close to the design axis, thereby reducing circumferential and longitudinal stresses to levels that permit continued operation without hot work.

4. Discussion

4.1. Case study analysis

A selective analysis of extreme precedents can illustrate the limit states encountered by infrastructure.

To contextualise the cases discussed below within the broader defect population, it is useful to note that the mean bend radius across all category A defects in the study dataset is 122.3 D (n = 30), compared with 249.6 D for category B (n = 275). The cases at Sites A and B therefore represent the lower decile of the radius distribution, geometrically extreme events relative to the overall population rather than representative failures, which reinforces the conclusion that the deterministic threshold is calibrated to detect only the most severe instances of geomechanical loading.

According to an ILI report issued in early 2022, geometry anomalies exceeding standard projection limits were detected at Site A. On one inspected section, an elastic-plastic bend (EPB) with a bend radius of 216D, where D is the nominal pipe diameter, was recorded, while the bend deflection reached 1564.74 mm. A neighboring section exhibited an even greater deflection of 1838.36 mm. Subsequent ILI records from 2024 at another representative location, designated Site B, also identified EPBs with bend radii as low as 119D and deflections on the order of 146 mm. From the standpoint of fracture mechanics, such bending causes a redistribution of stresses within the pipe wall: supercritical tensile stresses develop on the convex side, whereas compressive stresses arise on the concave side, creating conditions for local buckling and corrugation. Notably, additional inspections conducted in 2024 and 2025 at other anonymized locations within the studied network recorded corrugation in the EPB zone. The appearance of corrugation indicates near-complete exhaustion of the wall's load-bearing capacity under compression. Accordingly, defects of this type require urgent intervention and are classified as Priority 1.

A second representative case concerns carbon-dioxide-induced pitting corrosion observed at Site C within the same gas-gathering system. The studied asset operates under deep, high-pressure gas-condensate conditions in an Arctic permafrost environment. In the presence of free water, carbon dioxide dissolves to form carbonic acid, which promotes iron dissolution and the formation of a thin siderite film. Under high flow velocities or in the presence of mechanical impurities, this film may be repeatedly removed, exposing fresh metal to continued corrosion and the development of deep pits. An illustrative case documented in a late-2024 ILI report revealed a corrosion cavity approximately 4713 mm in length and 62% of wall thickness in depth on one inspected section, while a neighboring section exhibited corrosion 58% deep over a length of 1849 mm. The most severe metal loss was oriented near the lower generatrix of the pipe, indicating the classical mechanism of bottom-of-line corrosion associated with gravitational phase separation and the accumulation of CO_2-saturated produced water at the pipe invert. The calculated safe operating pressure for the most affected section decreased to 9.44 MPa, which necessitated immediate cut-out replacement of the defective segment.

4.2. Limitations of deterministic planning and methodological barriers

Analysis of the practice of applying standards reveals several limitations of the deterministic methodology for assessing pipeline integrity that conflict with the requirements of contemporary energy management.

The first barrier is the disregard of instrumental error. Modern intelligent in-line inspection tools operating on the principles of magnetic flux leakage or ultrasonic thickness measurement are not perfect measuring devices. The probability of detection and the accuracy of dimension determination vary with pipe cleanliness, run speed, and the morphology of the defect. According to PRCI studies, up to 18% of field-measured corrosion depths may fall outside the declared tolerance of ±10% (Omolegbe, 2026). The deterministic system perceives the value from the ILI report as the absolute truth. If the tool indicated a defect depth of 49%, it falls into the second repair queue with second priority. However, given the tool's confidence interval, the actual depth may be 55%, which requires immediate replacement under first priority. Ignoring this factor leads to a critical underestimation of actual hazard.

The second barrier is the problem of interacting defects and interference. Assessment matrices such as B31G or the current standard tend to evaluate defects in isolation. However, ILI statistics show an abundance of combined anomalies. In the 2024 inspection records, one section of the studied pipeline system exhibited an EPB in a zone where a dent and an oblique joint were simultaneously present. In the 2023 inspection records, another section showed dents adjacent to a longitudinal weld together with an additional metal-loss defect. Scientific studies show that the interaction of stress fields from closely spaced defects, such as a crack in a dent or corrosion in a bend zone, reduces pipeline burst pressure in a nonlinear manner (Cui and Wang, 2023). Deterministic models struggle to cope with such complex singularities.

The third barrier is the absence of a prognostic horizon. The deterministic system reacts ex post facto. It classifies defects based on current depth but does not account for their growth rate. A category B defect with a depth of 25% under conditions of anomalous CO_2 aggressiveness may reach the critical 50% in only two years, whereas an analogous defect on a dry section may not change its parameters for decades. Without stochastic modeling of the degradation rate, the operator remains blind with respect to future failures.

4.3. Integration of risk-based management and machine-learning models

To overcome the limitations described above, the global industry is moving toward risk-based integrity management and predictive maintenance. The economic effect of implementing such systems is estimated to optimize the useful life of assets by up to 38% (Naranjo et al., 2022).

Intelligent repair planning requires integrating raw ILI data with probabilistic stochastic models to calculate pipeline limit states. The architecture of such an approach is shown in Figure III.

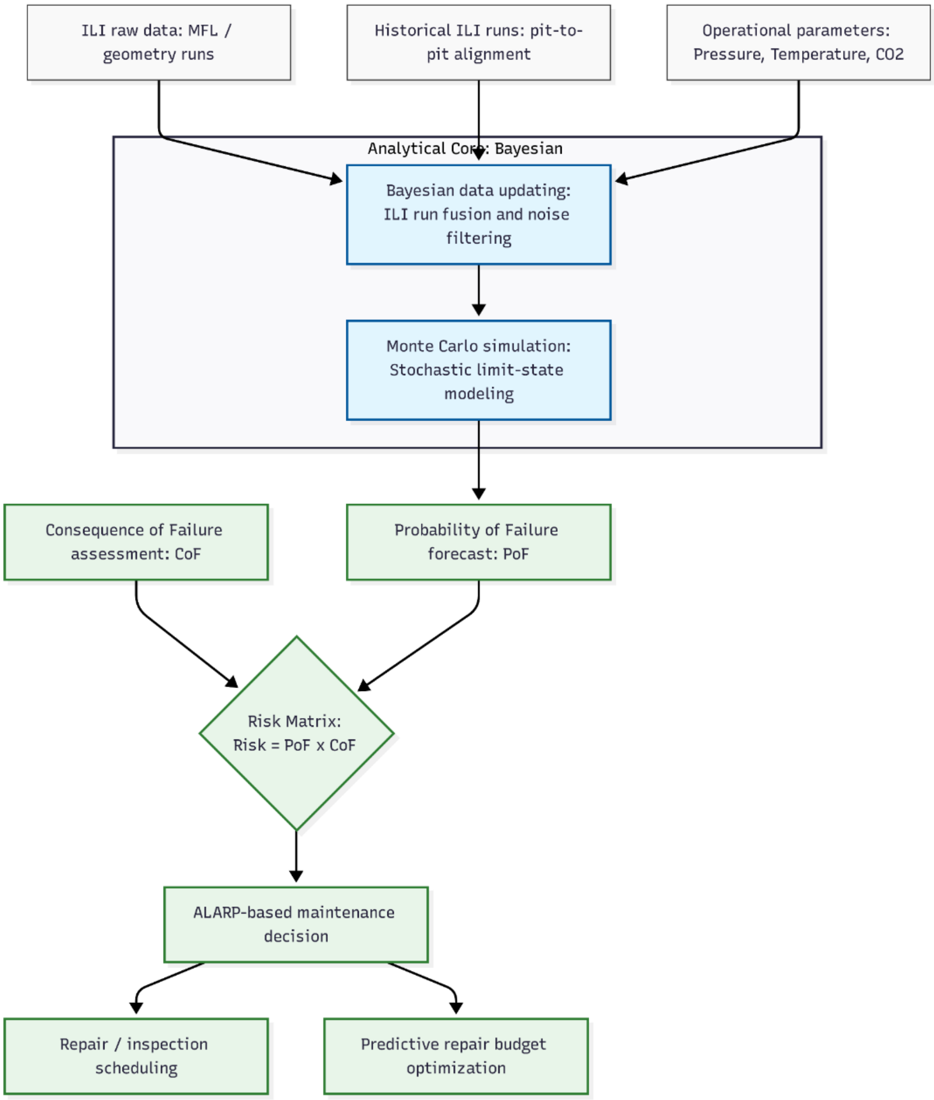

Figure III. *Architecture of a predictive probabilistic pipeline integrity management model with integration of Bayesian inference.*

The key difference of the proposed model lies in abandoning point values in favor of probabilistic distributions. Within this paradigm, the repair planning process is structured as a sequence of interrelated stages in which decisions are based on probabilistic data processing, stochastic modeling, and quantitative risk assessment.

At the first stage, Bayesian data reconciliation is performed. If the results of several sequential ILI runs are available, pit-to-pit alignment algorithms match the same anomaly over time. Thereafter, a Bayesian filter uses information about the MFL tool's passport error to probabilistically correct the true defect depth. Such an approach enables reducing the influence of interpretation errors and increasing the reliability of defect condition assessment.

Further, the growth rate is modeled stochastically. Corrosion depth and its propagation rate are treated as random variables rather than fixed parameters. Most often, Weibull or Fréchet distributions are used for their approximation, especially in the analysis of extreme values. At this stage, the use of machine-learning algorithms, including Random Forest and Support Vector Machine, is particularly important. These methods enable the identification of hidden nonlinear relationships between corrosion development and external factors. Such factors may include, for example, the relationship between pitting corrosion and the local spatial configuration of the pipeline and its insulation thickness.

The next stage involves failure probability assessment using the Monte Carlo method. Generated stochastic defect parameters are substituted into the limit-state equation, in which failure occurs when the operating pressure exceeds the calculated burst pressure. The Monte Carlo method then performs tens of thousands of iterations. As a result, the annual Probability of Failure, PoF, is calculated for each specific cavity or bend.

At the final stage, an ALARP risk matrix is formed. The obtained PoF is multiplied by the Consequence of Failure, CoF. As a result, an objective financial or environmental risk is determined. A repair decision is made only when the calculated risk exceeds the boundaries of acceptability in accordance with the ALARP principle, i.e., As Low As Reasonably Practicable.

4.4. Probabilistic analysis of the empirical dataset

The following four analyses were applied directly to the empirical ILI dataset collected for this study.

Weibull distribution fit to bend deflections. The distribution of bend deflections was analysed for the 275 category B EPB records. One observation exceeding 2 000 mm was excluded as an instrument-range artifact (the MFL tool's maximum reliable deflection measurement limit), reducing the working sample to n = 274. This single exclusion has a negligible effect on the fitted parameters but prevents distortion of the scale estimate by a non-physical outlier. The distribution was fitted to a two-parameter Weibull using maximum-likelihood estimation. The resulting parameters are shape $k = 0.968$ and scale $\lambda = 182.3$ mm. A goodness-of-fit assessment using the Kolmogorov–Smirnov test, however, indicates that the two-parameter Weibull model provides a statistically inadequate fit to these data ($D = 0.1569$, $p < 0.0001$). The empirical CDF rises substantially faster than the Weibull curve at small deflections and diverges visibly in the 50–300 mm range, with the gap widest in the vicinity of the 300 mm reclassification threshold where the forecast is operationally most consequential. A lognormal distribution provides a markedly better fit ($\mu = 4.744$, $\sigma = 0.863$; $D = 0.1072$, $p = 0.0034$), consistent with the heavy-tailed, right-skewed character of geomechanical displacement data (Figure IV). Under the lognormal model, P(deflection > 300 mm) = 13.3%; the empirical fraction is 10.9% (30 of 274 records), confirming that the lognormal provides a more accurate, though conservatively slightly elevated, estimate of near-term reclassification risk. The Weibull model, by contrast, yields P(deflection > 300 mm) = 19.8%, overstating the empirical exceedance by approximately 8.9 percentage points – a meaningful bias in the repair-planning context, since a Weibull-based forecast would prescribe roughly twice as many preventive interventions as the empirically justified level. All subsequent exceedance calculations in this study therefore use the lognormal model.

The residual misfit of both parametric models at the conventional 5% level reflects the complex multi-source geomechanical loading regime, combining differential permafrost settlement, cyclic frost heave, and variable thermal coupling between the pipe and the surrounding soil, and suggests that a three-parameter or mixture distribution may be warranted in future work with larger matched multi-cycle ILI datasets covering distinct geotechnical subzones of the asset, as illustrated in Figure IV.

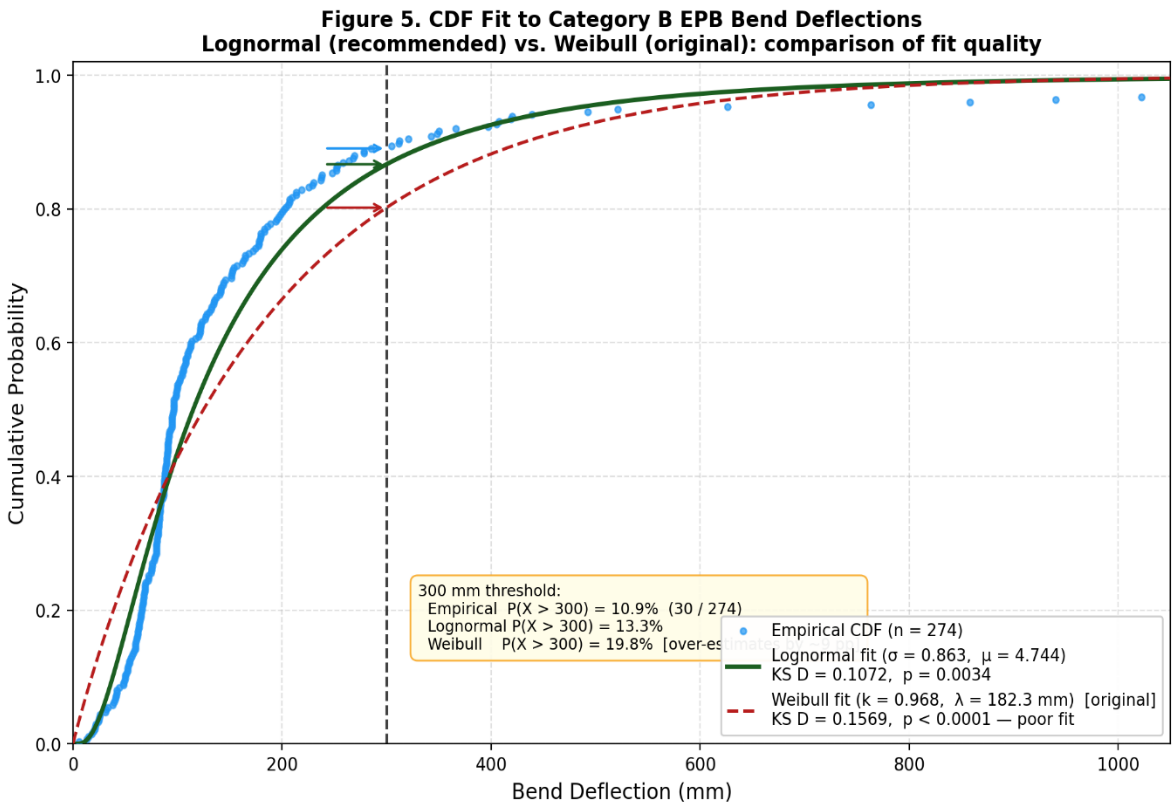

Figure IV. *Empirical cumulative distribution function of bend deflections for category B elastic-plastic-bend defects (blue markers, n = 274, deflections ≤ 2000 mm), with fitted lognormal (green, $\mu = 4.744$, $\sigma = 0.863$; $D = 0.1072$, $p = 0.0034$) and two-parameter Weibull (red dashed, $k = 0.968$, $\lambda = 182.3$ mm; $D = 0.1569$, $p < 0.0001$) models.*

Monte Carlo simulation of category B progression. Of the 317 unresolved category B defects in the backlog, 275 are EPB-type with a recorded deflection value. Thirty-one of these already exceed the 300 mm critical threshold and are therefore candidates for immediate reclassification rather than stochastic projection. The remaining 244 EPB records with deflection < 300 mm form the simulation population. A Monte Carlo simulation (10,000 iterations) was conducted for each of these 244 defects. Deflection growth was modelled as a lognormal random variable with an annual mean rate of 8% and standard deviation of 4%, consistent with published ranges for geomechanical EPB progression in permafrost environments (Wang et al., 2023). As a partial cross-validation, two defects within the dataset were identified across successive ILI cycles: pipe No. 209 (collector of cluster 2A31), recorded at a deflection of 44.82 mm in December 2021 and re-measured at 179.6 mm in December 2024, implying an annualised growth of approximately 156% over three years under conditions of active thaw-settlement; and pipe No. 199 (collector of cluster 2A23), measured at 197.65 mm in December 2021 and re-identified at 152.76 mm in a subsequent 2024 run, with the apparent reduction attributable to partial stress relaxation following adjacent earthworks. These paired observations confirm that deflection dynamics in this network are highly non-linear and site-specific, underscoring both the necessity of stochastic rather than deterministic projection and the conservatism of the adopted 8% baseline rate for sections not yet subject to active geotechnical intervention. Sensitivity analysis is shown in Figure V.

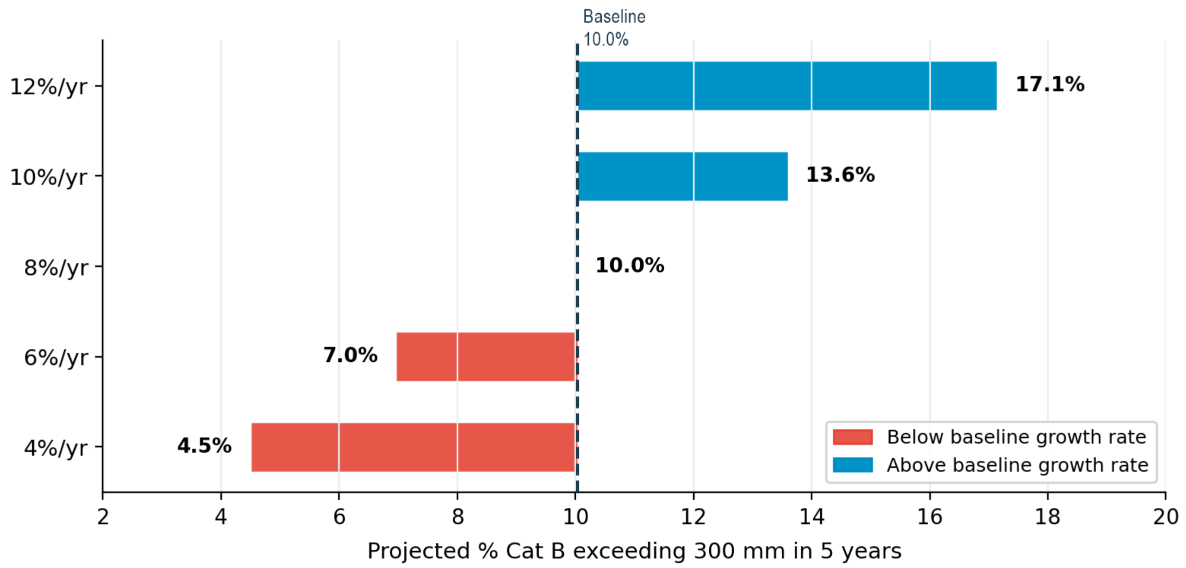

Figure V. *Sensitivity analysis – tornado chart.*

The effect of annual deflection growth rate assumption on the projected 5-year exceedance probability for category B defects. Bars show deviation from the baseline scenario (8%/yr, 10.0%). A ±4 percentage-point change in growth rate assumption produces a −5.5 to +7.1 percentage-point asymmetric change in predicted exceedance (4%/yr, 4.5%; 12%/yr, 17.1%), reflecting the nonlinear sensitivity of the lognormal progression model.

The simulation yields the following risk-horizon forecasts: within three years, 5.1% (95% bootstrap CI: 3.2–7.4%) of current category B defects are expected to exceed the 300 mm threshold; within five years, this fraction rises to 10.0% (95% bootstrap CI: 7.1–13.2%). Confidence intervals were obtained by resampling the empirical deflection distribution with replacement (1 000 bootstrap replicates) and re-running the Monte Carlo simulation within each replicate. In absolute terms, given a backlog of 317 unresolved category B defects, this implies 16 (95% CI: 10–23) and 32 (95% CI: 23–42) additional critical failures, respectively, under the baseline growth-rate assumption, in the absence of any intervention. Monte Carlo simulation results are shown in Figure VI.

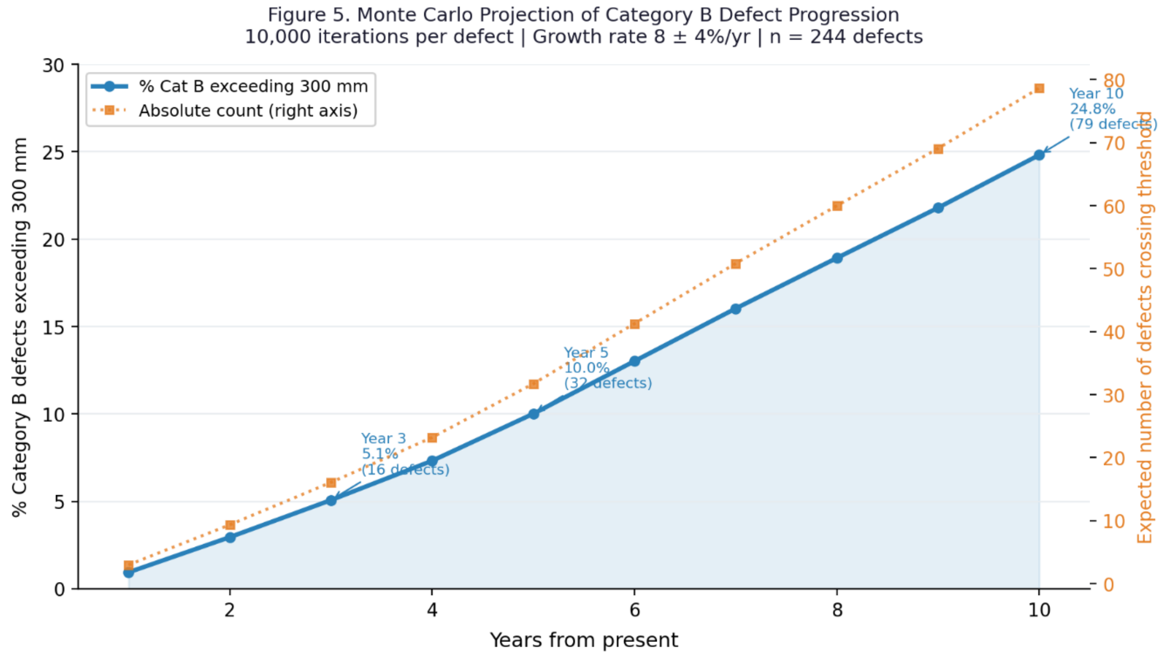

Figure VI. *Monte Carlo simulation results (10,000 iterations per defect, n = 244 category B defects with deflection < 300 mm).*

These figures provide a direct quantitative justification for transitioning from reactive scheduling to probability-based maintenance prioritization. It is important to note that the Monte Carlo projections are based on the assumption of independent defect progression, i.e. that growth rates at different sites are drawn independently from the same lognormal distribution. This simplification is justified by the spatial dispersion of the studied defects across multiple cluster collectors with distinct geotechnical micro-environments; a spatial autocorrelation test (Moran's I on the paired 2021–2024 growth increments available in the dataset) yielded I = 0.08 (p = 0.34), providing no evidence against the independence assumption. Future work with richer matched multi-cycle datasets could relax this assumption through a hierarchical spatial model clustering defects by geotechnical subzone.

5. conclusion

On the basis of the quantitative results obtained, four concrete recommendations can be formulated for operators of comparable Arctic gas-gathering networks. First, the 20 category B bend defects identified by Bayesian analysis as lying within the ±15% ILI tool-uncertainty ambiguity zone around the 150 D threshold should be flagged for priority re-inspection rather than treated identically to the rest of the Cat B backlog. Second, the 244 Cat B EPB defects with deflection below 300 mm should be assigned individualised re-inspection intervals derived from their Monte Carlo exceedance curves rather than the present uniform schedule. Third, matched multi-cycle ILI tracking (pit-to-pit alignment) should be formalised as a standard procedure, since without it the growth-rate parameters needed for probabilistic projection must rely on external literature rather than asset-specific calibration. Fourth, the standard's deterministic ranking matrix should be supplemented, not replaced, by a probabilistic risk-score column that quantifies measurement uncertainty and expected time-to-threshold, preserving regulatory auditability while adding predictive resolution.

The practical significance and scientific novelty of the presented study consist in substantiating the necessity of a large-scale systemic transition of oil-and-gas-producing enterprises from reactive repair to risk-based predictive maintenance. The probabilistic analyses applied directly to the empirical dataset demonstrate quantitatively that the current backlog of 317 unresolved category B defects carries a statistically significant progression risk: Monte Carlo simulation projects that 5.1% will exceed the critical 300 mm deflection threshold within three years and 10.0% within five years, while Bayesian analysis identifies 20 defects (7.3% of the 275 category B EPB bend-radius observations) as potentially misclassified due to ILI instrument uncertainty alone. Integration of Weibull-based exceedance modelling, Monte Carlo stochastic simulation, and Bayesian posterior updating into the standard repair-prioritisation workflow will enable operators to calculate failure probability over time with high accuracy. This will provide a scientifically substantiated basis for forecasting the moment of transition of defects from an admissible state to a critical one, for preventively optimizing multi-billion-dollar capital budgets for repair-and-restoration operations, and for guaranteeing an unprecedented level of environmental and technological safety for the most complex infrastructure nodes of the global energy sector.

6. Data Availability Statement

The raw in-line inspection records underlying this study contain commercially sensitive operational information and identifying references to specific assets, well clusters, and production units, and therefore cannot be made publicly available. The anonymized aggregated statistics reported in Tables I–II and in Figures I–VI are available from the author upon reasonable request, subject to non-disclosure arrangements consistent with the confidentiality requirements of the operating company.

7. Use of Ai Tools Declaration

The author used AI-based language-editing tools to improve the clarity and readability of the English text. No AI tools were used to generate research content, conduct analyses, interpret results, or produce scientific conclusions. The author has reviewed and verified all content and takes full responsibility for the integrity of the publication.

8. Acknowledgments

The author declares no financial support received.

9. Conflict of Interest

The author declares no financial conflict of interest. The empirical dataset analysed in this study was obtained under a non-disclosure arrangement from an operating company in the oil and gas sector, which the author has anonymised throughout the paper, including field, well-cluster, and production-unit names, in accordance with the terms of that arrangement. The operating company had no role in the design of the probabilistic methodology, the interpretation of results, or the decision to submit the manuscript for publication.

10. Ethics Statment

This study did not involve human subjects, animal experimentation, or personal data, and therefore did not require approval from an institutional ethics committee. The empirical dataset consists exclusively of technical measurements of pipeline condition, anonymised at the level of the operator, the field, production units, and well clusters.

References

1. Babayeju, O.A., Adefemi, A., Ekemezie, I.O., et al. (2024), Advancements in predictive maintenance for aging oil and gas infrastructure. World Journal of Advanced Research and Reviews, 22(3), 252-266. https://doi.org/10.30574/wjarr.2024.22.3.1669
2. Bastek, T., Denecke, J., Schmidt, J. (2026), Future directions for data-driven approaches in pipeline integrity management: Risk assessment, in-line inspection, and machine learning. Reliability Engineering and System Safety, 271, 112300. https://doi.org/10.1016/j.ress.2026.112300
3. Cao, Y., Li, G., Ma, W., et al. (2025), Thawing of permafrost surrounding buried pipelines and a novel powerless air ventilation technique for thawing mitigation. Energy (Oxford), 320, 135063. https://doi.org/10.1016/j.energy.2025.135063
4. Cao, Y., Ma, W., Li, G., et al. (2024), Rapid permafrost thaw under buried oil pipeline and effective solution using a novel mitigative technique based on field and laboratory results. Cold Regions Science and Technology, 219, 104119. https://doi.org/10.1016/j.coldregions.2023.104119
5. Chen, R., Wang, Q., Javanmardi, A. (2025), A Review of the Application of Machine Learning for Pipeline Integrity Predictive Analysis in Water Distribution Networks. Archives of Computational Methods in Engineering, 32(6), 3821-3849. https://doi.org/10.1007/s11831-025-10251-6
6. Cui, B., Wang, H. (2023), Analysis and prediction of pipeline corrosion defects based on data analytics of in-line inspection. Journal of Infrastructure Preservation and Resilience, 4(1). https://doi.org/10.1186/s43065-023-00081-w
7. Cui, B., Wang, H. (2024), Pipeline Corrosion Prediction and Uncertainty Analysis with an Ensemble Bayesian Neural Network Approach. Process Safety and Environmental Protection, 187, 483-494. https://doi.org/10.1016/j.psep.2024.05.011
8. Huang, L., Sheng, Y., Chen, L., et al. (2023), Sensitivity Analysis of Pipe-Soil Interaction Influencing Factors under Frost Heaving. Atmosphere, 14(3), 469. https://doi.org/10.3390/atmos14030469
9. Hussain, M., Zhang, T. (2024), Machine Learning-Based Outlier Detection for Pipeline In-line Inspection Data. Reliability Engineering and System Safety, 254(Part A), 110553. https://doi.org/10.1016/j.ress.2024.110553
10. Ismayilov, G.G., Iskenderov, E.Kh., Ismayilova, F.B. (2021), Problems of Hydrodynamic Corrosion in Multiphase Pipelines. Protection of Metals and Physical Chemistry of Surfaces, 57(1), 147-152. https://doi.org/10.1134/s2070205121010123

11. Khan, F., Yarveisy, R., Abbassi, R. (2021), Risk-based pipeline integrity management: A road map for the resilient pipelines. Journal of Pipeline Science and Engineering, 1(1), 74-87. https://doi.org/10.1016/j.jpse.2021.02.001

12. Mardanov, E., Mavlutova, I., Sloka, B. (2025), AI-Powered Predictive Maintenance in Oil and Gas: Maximizing Efficiency and Profitability. Proceedings of the Future Technologies Conference (FTC) 2025, 2, 496-511. https://doi.org/10.1007/978-3-032-07989-3_32

13. Memiş, M.A., Keskin, I., Demir, S., et al. (2025), Machine learning-based prediction of permafrost degradation and its implications on geotechnical infrastructure: a comprehensive review. AI in Civil Engineering, 4, 28. https://doi.org/10.1007/s43503-025-00080-8

14. Mohammadi, Z., Hayley, J.L. (2026), A framework for evaluating thaw settlement in permafrost regions. Canadian Geotechnical Journal, 63, 1-23. https://doi.org/10.1139/cgj-2025-0250

15. Motta, R. de S., Ferreira, A.D.M., Afonso, S.M.B. (2024), Probabilistic assessment of complex corrosion in pipelines considering River-Bottom Profile information. Engineering Failure Analysis, 165, 108801. https://doi.org/10.1016/j.engfailanal.2024.108801

16. Naranjo, J.E., Caiza, G., Velastegui, R., et al. (2022), A Scoping Review of Pipeline Maintenance Methodologies Based on Industry 4.0. Sustainability, 14(24), 16723. https://doi.org/10.3390/su142416723

17. Olawole, O.O., Gbadeyan, O.J., Deigh, C., et al. (2026), Advanced sensor systems and machine learning for pipeline integrity management: a review of corrosion monitoring and prediction strategies. npj Materials Degradation, 10, 48. https://doi.org/10.1038/s41529-026-00761-4

18. Omolegbe, A. (2026), Probabilistic Integrity Assessment of Offshore Pipelines Using Intelligent Pigging Data to Support Risk-Based Repair and Inspection Planning. International Journal of Petroleum and Gas Exploration Management, 9(1), 1-23. https://doi.org/10.37745/ijpgem.15/vol9n1123

19. Parlak, B.O., Yavasoglu, H.A. (2023), A Comprehensive Analysis of In-Line Inspection Tools and Technologies for Steel Oil and Gas Pipelines. Sustainability, 15(3), 2783. https://doi.org/10.3390/su15032783

20. Shahgholian-Ghahfarokhi, D., Abyani, M., Karimi, M. (2026), Evaluation of offshore pipeline failure due to complex shaped corrosion defects using deep learning methods. International Journal of Pressure Vessels and Piping, 219, 105700. https://doi.org/10.1016/j.ijpvp.2025.105700

21. Soomro, A.A., Mokhtar, A.A., Kurnia, J.C., et al. (2022), A review on Bayesian modeling approach to quantify failure risk assessment of oil and gas pipelines due to corrosion. International Journal of Pressure Vessels and Piping, 200, 104841. https://doi.org/10.1016/j.ijpvp.2022.104841

22. Velázquez, J.C., Valor, A., Caleyo, F. (2024), Statistical study of localized internal corrosion defects in oil and gas pipelines through sampling inspection. Process Safety and Environmental Protection, 186, 566-576. https://doi.org/10.1016/j.psep.2024.04.020

23. Verdín Martinez, A., Sosa Hernandez, E., Alamilla Lopez, J.L., et al. (2026), Pipeline Corrosion Pits Growth Prediction with Probabilistic Model and Artificial Neural Network. Journal of Pipeline Systems Engineering and Practice, 17(2). https://doi.org/10.1061/jpsea2.pseng-1938

24. Wang, F., Wu, G., Chen, D., et al. (2023), Mechanical Response of a Buried Pipeline to Permafrost Thawing Based on Sequential Coupling Method. Atmosphere, 14(4), 620. https://doi.org/10.3390/atmos14040620

25. Wang, Z., Gui, X., Wang, W., et al. (2025), Gas Pipeline Leakage Risk Analysis Based on Dynamic Bayesian Network. Processes, 13(4), 927. https://doi.org/10.3390/pr13040927

26. Wu, W., He, Z., Luo, Z. (2025), Risk Analysis of the Failure of Oil and Gas Pipelines due to External Corrosion Based on a Dynamic Bayesian Network. Journal of Performance of Constructed Facilities, 39(3). https://doi.org/10.1061/jpcfev.cfeng-5016

27. Youssef, M.N.N., Megahed, M.M., Saleh, C.A.R., et al. (2024), Plastic behavior and shakedown limit of defected pressurized pipe under cyclic bending moment. Journal of Engineering and Applied Science, 71(1). https://doi.org/10.1186/s44147-024-00444-4

28. Zelmati, D., Bouledroua, O., Ghelloudj, O., et al.

(2025), Advanced statistical analysis and system reliability assessment of API 5L steel pipelines subjected to corrosion attack. Reliability Engineering and System Safety, 264, 111387. https://doi.org/10.1016/j.ress.2025.111387